Self-Assembly

DOI: 10.1002/anie.201201796

Ribbons, Vesicles, and Baskets: Supramolecular Assembly of a Coil–Plate–Coil Emeraldicene Derivative**

*Mingfeng Wang, Ali Reza Mohebbi, Yanming Sun, and Fred Wudl**

Supramolecular assembly of π-conjugated molecules is important for organic optoelectronic devices where the intermolecular interaction and ordering at the different length scales determine the electronic properties.[1] In molecular semiconductors, π-conjugated molecules are the building blocks of solid-state architectures instead of atoms as in traditional semiconductors. While atoms are linked covalently in crystalline inorganic semiconductors, relatively weak π–π interaction and van der Waals forces play a crucial role in defining the electronic properties in molecular semiconductors.[2]

Conjugated molecules, depending on their molecular structures and processing conditions, self-assemble into a variety of nano/microscale structures, such as spheres,[3] wires,[4] ribbons,[5] tubes,[6] helices,[7] disks,[8] sheets,[9] toroids,[4b,10] barrels,[11] vesicles,[12] and honeycombs.[13] In particular, rod–coil molecules, consisting of rigid rod and flexible coil segments, are one of several self-assembling building blocks for creating well-defined supramolecular structures in selective solvents for the flexible coil segments.[1a,5e,14] In contrast to coil–coil systems,[15] the rod–coil systems can form well-ordered structures even at relatively low molecular weights of each block, because the stiff rod-like conformation of the rod segments imparts orientational organization.[16]

Herein we extended the concept of the rigid segment to a plate endowed with π–π attractive interactions and report the colloidal self-assembly of a coil–plate–coil emeraldicene derivative **1**, synthesized by Mohebbi et al. using a modified literature procedure.[17] The molecular structure of **1** is shown in Figure 1a. Our initial objective was to reveal the self-assembly behavior of this novel coil–plate–coil emeraldicene derivative, in comparison with those of conventional rod–coil molecules. We also characterized the charge transport properties of the elongated self-assembled structures (i.e. ribbons) to demonstrate how the supramolecular organization of the π-conjugated moieties determines the inherent electronic properties (see below).

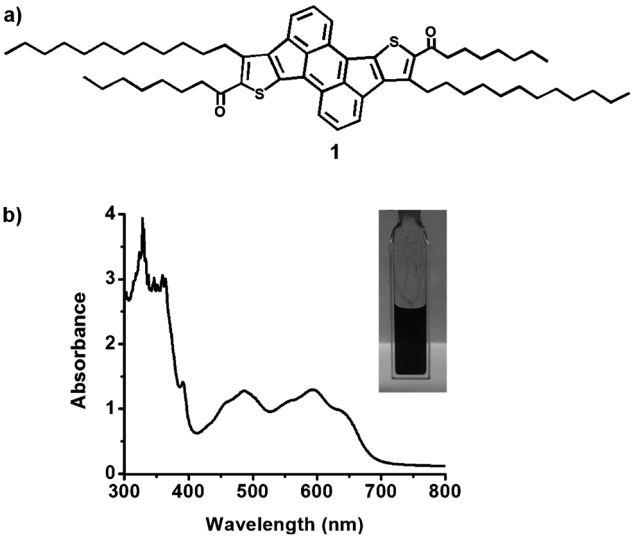

Figure 1. a) The molecular structure of the coil–plate–coil emeraldicene derivative **1**. b) The UV/Vis absorption spectrum of **1** in THF. The inset shows a digital photograph of the solution in THF at 2.0 mg mL^{-1}.

Emeraldicenes are heteroaromatic π-conjugated molecules with extended π-electron structures and high electron affinities, and have potentials in optoelectronic applications.[18] These molecules, depending on the alkyl substituents, form face-to-face and/or edge-to-face π–π stacking motifs in single crystals.[17b] Nevertheless, it remains unknown whether such a π–π stacking interaction assists the formation of micro/nanostructures in solvents.

The covalent attachment of dodecyl and octyl chains to emeraldicenes led to increased solubility of **1**, compared to that of the nonsubstituted emeraldicenes. Differential scanning calorimetry (DSC) measurement of **1** gives a melting point at 118 °C, accompanied by a small shoulder at 108 °C in the heating cycle (Figure S1 in the Supporting Information). The suspension of **1** in THF shows a broad absorption band in the UV/Vis range, with an onset at 690 nm (Figure 1b). Similar absorption feature was observed in chloroform.

[*] Dr. M. Wang, Dr. A. R. Mohebbi, Prof. F. Wudl
Department of Chemistry and Biochemistry
Center for Polymers and Organic Solids
and Materials Research Laboratory
University of California
Santa Barbara, CA 93106-6105 (USA)
E-mail: wudl@chem.ucsb.edu
Dr. Y. Sun
Department of Physics
and Center for Polymers and Organic Solids
University of California
Santa Barbara, CA 93106-6105 (USA)

[**] We thank Dr. Stephan Kraemer and Mark Conish for the help in electron microscopy and Dr. Mary Raven for the help in fluorescence microscopy. We are grateful to Prof. A. J. Heeger for helpful discussion. M.W. thanks the support of Natural Sciences and Engineering Research Council of Canada for the support of a Postdoctoral Fellowship (Grant No. PDF-373502-2009). A.R.M. thanks financial support (Grant No. DE-FG02-08ER46535) from Department of Energy.

Supporting information for this article is available on the WWW under http://dx.doi.org/10.1002/anie.201201796.

When **1**, isolated from dichloroethane, was dissolved in tetrahydrofuran (THF) at a concentration of 2.0 mg mL^{-1}, a visually transparent deep-blue solution was obtained. After standing in a sealed vial at room temperature overnight, a suspension of tiny particles was observed, thus suggesting the aggregation of **1**. Under excitation with 520–550 nm light, red-fluorescent fibrillar aggregates were observed by using a fluorescence microscope (Figure S2 in the Supporting Information). These fibrillar aggregates, stored over one year in the dark in a capped and sealed vial, still retained their morphologies and optical properties, thereby implying that these structures are thermodynamically stable.

When a solution of **1** (2.0 mg mL^{-1}) in THF was drop-cast on a precleaned silicon substrate and subsequently dried in air at room temperature, flexible ribbons with a high aspect ratio were observed by scanning electron microscopy (SEM; Figure 2a,b). These ribbons appear relatively uniform in width ((0.9 ± 0.2) μm) and in thickness ((0.15 ± 0.05) μm,

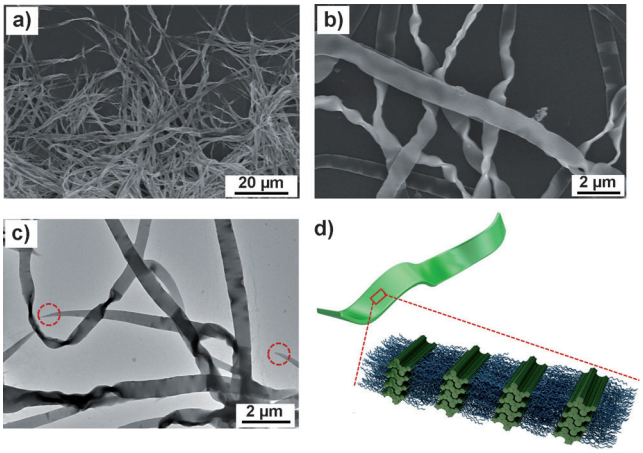

Figure 2. a,b) SEM images and c) TEM image of **1** in films drop-cast from an aliquot of 2.0 mg mL^{-1} in THF. The dashed cycles in (c) highlight the ends of some nanoribbons. d) Schematic presentation of the molecular packing of **1** along the nanoribbon.

measured by atomic force microscopy (AFM; Figure S3 in the Supporting Information). The twisting feature of the ribbons allows one to see their edges by SEM (Figure S4 in the Supporting Information), which gives an average thickness of (0.18 ± 0.03) μm. The ribbons extend in one dimension up to tens of micrometers or even longer. In high-resolution SEM images (Figure 2b), the corrugating feature is obvious for most of these ribbons, reminiscent of flat Asian noodles. Similar morphology was observed by transmission electron microscopy (TEM; Figure 2c) in a film formed from the same solution on a carbon-coated copper grid. In some areas, labeled by dashed circles in Figure 2c, the ends of the ribbons can be discerned, where the ribbons become sharper and focus gradually to a point at the end. The electron diffraction pattern (Figure S5 in the Supporting Information) indicates that the ribbons are crystalline, with the π–π stacking aligned along the long axis of the ribbons (Figure 2d). A proposed packing model of **1** along the individual ribbons is presented in Figure 2d. We believe that the π–π interaction between the aromatic core of **1**, as demonstrated in the single-crystal structures of emeraldicene derivatives,[17b] provides a major driving force to direct the formation of the ribbons. This conclusion is also supported by the following charge transport measurements.

The elongated supramolecular structures of the ribbons described above raised our interest to characterize their charge transport properties in field-effect transistor (FET) devices. The devices were fabricated by drop-casting an aliquot of **1** in THF (2.0 mg mL^{-1}) onto SiO_2/Si substrates that were prepatterned with interdigitated gold electrodes, then coated with a monolayer of *n*-octyltrichlorosilane, and subsequently dried in air at room temperature. From the saturated regime of the *I–V* transfer plots, the estimated hole mobility was 2.1×10^{-6} cm^2 V^{-1} s^{-1}, when assuming a full coverage of the sample in the channel (5 μm in length) between the two electrodes (Figure S6 in the Supporting Information). Though the mobility measured here is comparable to other 1D self-assembled nanostructures of π-conjugated molecules,[19] it should be noted that the actual mobility was underestimated here since the channels were only partially (ca. 40%) covered by the sample. A more accurate measurement of a single ribbon in the future should give a higher mobility than the value estimated above.[4f]

Interestingly, after the film was annealed at 120 °C in N_2 atmosphere for five minutes, the SEM image (Figure S6 in the Supporting Information) shows that the ribbons collapsed into irregular smooth domains. The *I–V* transfer plot (Figure S6) shows that the hole mobility of the film decreased to 5.2×10^{-10} cm^2 V^{-1} s^{-1}. Such a dramatic decrease of the charge-carrier mobility upon the morphological change demonstrates that the well-defined supramolecular organization of **1** and the oriented π–π stacking in the ribbons play a crucial role in determining the electronic properties in devices.

Solvent plays an important role in the formation of the well-defined aggregates. For example, when the solvent was changed to chloroform, in contrast to THF, the solution with the same concentration (i.e. 2.0 mg mL^{-1}) remained transparent. No aggregation was observed by using an optical microscope even after the solution was stored in a capped and sealed vial in the dark for up to one year. Furthermore, when a chloroform solution of **1** (2.0 mg mL^{-1}) was drop-cast on a silicon substrate, irregular smooth films without defined morphologies (Figure S7 in the Supporting Information) were observed by SEM. This result is consistent with the aggregation-free state of **1** in chloroform.

To understand the effect of concentration on the assembly of **1**, we prepared a solution at 0.2 mg mL^{-1} in THF and followed the same procedure as described above for SEM and TEM measurements. While **1** at 2.0 mg mL^{-1} formed ribbons over the whole silicon substrate (Figure 2), two domains with different morphologies formed in the film drop-cast from the 0.2 mg mL^{-1} solution (Figure 3). Figure 3a shows a low-magnification SEM image of the film where both networks of ribbons (Region 1, the edge of the film) and smaller-size discrete aggregates (Region 3, the center of the film) as well as the boundary (Region 2) can be discerned. The high-resolution SEM image (Figure 3b) of the boundary clearly shows the transformation from networks of ribbons to

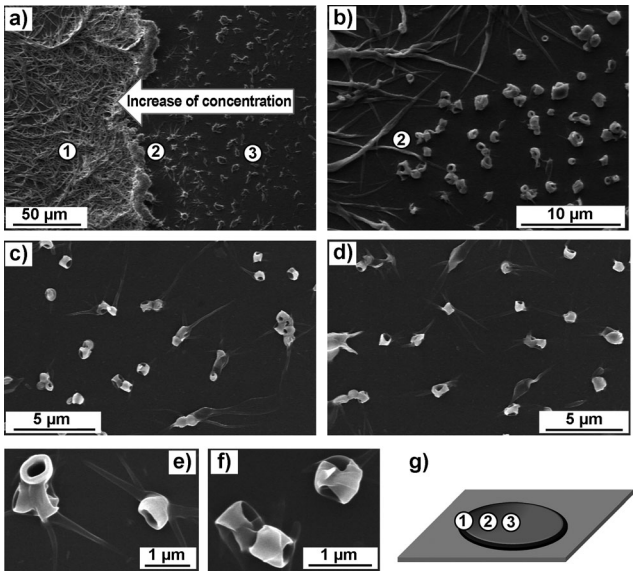

Figure 3. a–f) SEM images of **1** in films drop-cast from an aliquot of 0.2 mg mL^{-1} in THF. a) Low-magnification image where the two regions with different morphologies can be seen. b) Magnified image of the boundary between nanoribbons and nanobaskets. c, d) Representative images in Region 3, the center of the film. e, f) Structural details of the baskets formed in Region 3 are highlighted. g) Schematic presentation of Regions 1–3 caused by the "coffee-ring" effect in the film.

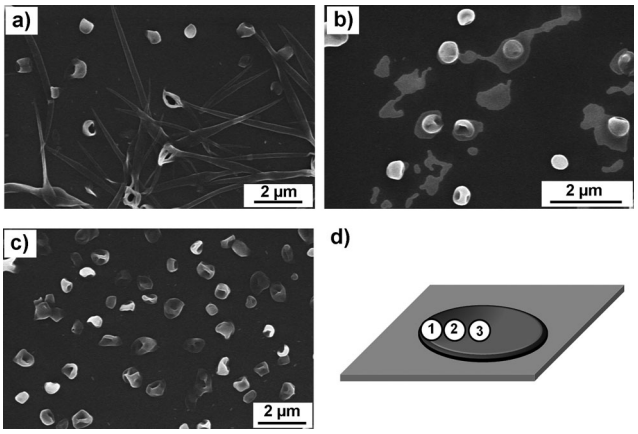

Figure 4. a–c) SEM images of **1** in films drop-cast from an aliquot of 0.5 mg mL^{-1} in THF. a) Region 1 (d) in the film, where ribbons, open-ended baskets, and shell-closed globules coexist. b) The central region (Region 3, (d)) of the film, where both globular aggregates and irregular pieces of sheets can be seen. c) The exclusive formation of collapsed vesicles in Region 2 of the film is shown. The collapsed feature of the globules under the high vacuum condition of the SEM measurement (Figure 5 b, c) proves the hollow nature of these aggregates, that is, vesicles. d) Schematic presentation of Regions 1–3 caused by the "coffee-ring" effect in the film.

discrete aggregates with varying sizes and shapes. Some detailed morphologies of the aggregates formed in Region 3 can be seen in representative high-resolution SEM images shown in Figure 3 c–f. In the center of the film (Region 3) the ribbons curved and self-wrapped into baskets with open ends. Some baskets have relatively thick walls and are open at only one end (Figure 3 e), while some (i.e. toroids) have relatively thin walls and remain open at both ends (Figure 3 f).

The structural characteristics of the baskets presented in Figure 3 d, e can be further discerned by TEM (Figure S8 in the Supporting Information). The relatively low-magnification image (Figure S8-a) shows the presence of partially deformed ribbon-like aggregates attached by baskets that appear darker in the image. The high-resolution TEM image (Figure S8-b) shows the interior structure of some basket-like aggregates, where the hollow feature and the open-ended structure can be seen. Furthermore, one can see that the wall of some baskets consists of double-layer or multilayer sheets, consistent with the results observed by SEM (Figure 3 e, f).

To identify the assembled structure of **1** at a concentration between 2.0 and 0.2 mg mL^{-1} in THF, as an example, we characterized a sample at 0.5 mg mL^{-1}. The SEM images of the film drop-cast from this solution on a silicon substrate are shown in Figure 4. In regions close to the edge of the film (Region 1, Figure 4 d), the coexistence of ribbons, open-ended baskets, and shell-closed capsules was observed (Figure 4 a). In contrast, in the central regions of the film (Region 3, Figure 4 b), capsules and irregular pieces of sheets were observed. In some regions (e.g. Region 2) between the center and the edge of the film, exclusive formation of discrete collapsed capsules was observed (Figure 4 c and Figure S9 in the Supporting Information). A size analysis of eighty capsules[20] gives an average diameter of (606 ± 182) nm. A more accurate size analysis of these capsules was difficult owing to the irregularity caused by the collapse of these hollow structures under high vacuum condition of the SEM measurement. Meanwhile, the collapsed feature of these capsules (Figure 4 b, c) proves the hollow nature of these aggregates, that is, vesicles.

We further characterized **1** at 0.5 mg mL^{-1} in THF by using confocal fluorescence microscopy. Here the sample was sealed in a capillary glass tube and then imaged in the wet state, thus the effect of solvent evaporation was avoided. The results (Figure S10 in the Supporting Information) indicate that the major population of the aggregates includes vesicles with relatively strong fluorescence, irregular sheets with relatively weak fluorescence, accompanied by a minor population of short ribbons.

Although the limited resolution of the optical microscope was not able to give the detailed structural characteristics of these aggregates in the wet state, the results above imply that the morphological transformation from the ribbons to vesicles occurred in solution upon dilution, that is, before the solvent evaporation. On the one hand, the aggregates formed in the central regions of the films (Figures 3 and 4), where the solvent evaporates faster than in the edges, are assumed to represent those in the solutions, although the possibility of kinetically trapped structures during solvent evaporation cannot be excluded. On the other hand, the formation of the ribbons at the edges of the films drop-cast from solutions with 0.2 or 0.5 mg mL^{-1} of **1** can be attributed to the "coffee-ring" effect:[21] liquid evaporating from the edge is replenished by liquid from the interior of the droplet. The concomitant edge evaporation leads to a concentration gradient where the material is more concentrated in the

edge than in the center of the film. Better controlled evaporative self-assembly of **1** at lower concentrations (e.g. 0.2–0.5 mg mL^{-1}), for example, in confined geometries,[22] may lead to more uniform supramolecular structures with defined morphologies, studies that are beyond this initial disclosure but will be subject of future studies.

The experimental results described above demonstrate that the size of the aggregates (from ribbons to vesicles and to baskets) decreases significantly as the concentration of **1** decreases from 2.0 to 0.2 mg mL^{-1}. The ultralong ribbons formed at 2.0 mg mL^{-1} represent an infinite aggregate with a rather large aggregation number (N). Given an average volume of 2.88 nm^3 for the individual molecule, N is 1.88×10^9 for a ribbon with a dimension of 0.9 μm in width, 0.15 μm in height, and 40 μm in length. For the vesicles formed at 0.5 mg mL^{-1}, in contrast, the aggregation number is much lower. For example, N is 4.47×10^6 for a vesicle with an outer radius of 0.3 μm and a thickness of 0.15 μm. According to the equation,[23]

$$\mu_N = \mu_\infty + \alpha k T/N^p \quad (1)$$

the decrease of the aggregation number (N) is associated with an increase of the mean interaction free energy per molecule (i.e. μ_N). This increase of μ_N is compensated by the elimination of the unfavorable rim energy of the ribbon by its closing up into a basket or a vesicle. In other words, these baskets and vesicles may represent thermodynamically stable structures at low concentrations in THF. However this is still a dynamic system and, even though the ribbons are visible in solution, it has been difficult to observe baskets in solution.

The morphological transformation pathway observed here is different from those of conventional amphiphilic molecules. For instance, the self-assembly of cetyltrimethylammonium bromide, upon a gradual increase of the concentration in water, typically evolves from free molecules to spherical micelles to cylindrical micelles to liquid crystalline phases.[24] For the self-assembly of diacetylenic lipids, Schnur et al.[25] reported a transformation pathway from large vesicles or lipid bilayer aggregates to ribbons to helices and to tubes, depending on the solvent and the temperature. The Bates research group[26] reported the self-assembly of a coil–coil diblock copolymer, polybutadiene-poly(ethylene oxide), which transited from isotropic worm-like micelles to nematic phase to hexagonal phase upon the increase of the polymer concentration in water.

In contrast to the well-established self-assembly of conventional amphiphilic molecules and coil–coil block copolymers, the self-assembly of rod–coil molecules remains less understood. Previous theoretical[27] and experimental[1a,5e,6a,9,11,14,19] studies illustrated how variation of molecular structures, such as the rod/coil fraction ratio and the segregation strength, as well as changing of the processing conditions (e.g. solvent, temperature) affect the self-assembly behavior. For instance, the Aida research group[6a] reported the transformation from bilayer tapes to helices to tubes, depending on the solvent, in the self-assembly of an amphiphilic hexa-*peri*-hexabenzocoronene derivative. But the effect of concentration on the self-assembly was not reported.

Our electron microscopy results have revealed a unique transformation pathway from nanometer-thin ribbons to vesicles and to toroids/baskets in the self-assembly of the coil–plate–coil emeraldicene derivative **1** (Figure 5), upon decrease of the concentration in THF. In particular, a unique intermediate assembled structure has been identified: nanoscale baskets, which are formed by curved and self-wrapped nanometer-thin ribbons. Moreover, the elongated supramolecular organization of **1** and the oriented π–π stacking in the ribbons play a crucial role in determining the charge transport properties in thin films. The self-assembly of this π-conjugated molecule enables a bottom-up strategy to construct complex nano/microstructures with desired optoelectronic properties.

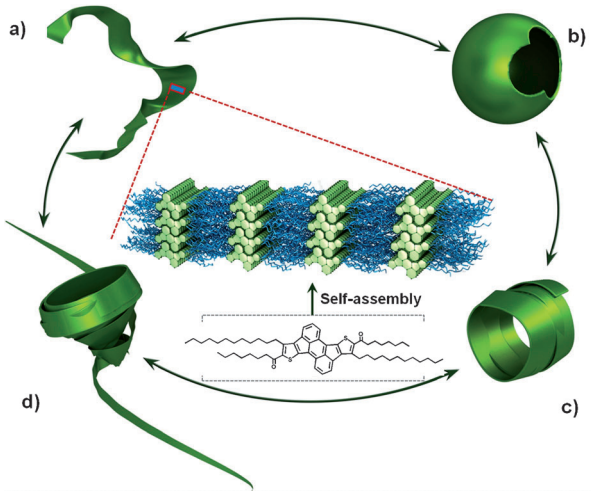

Figure 5. Schematic representation of the morphological transformation from a) nanometer-thin ribbons to b) vesicles to c) toroids and to d) baskets formed by the coil–plate–coil emeraldicene derivative **1**.

Received: March 6, 2012
Revised: May 15, 2012
Published online: June 6, 2012

Keywords: conjugated molecules · nanostructures · self-assembly · supramolecular chemistry · vesicles

[1] a) F. J. M. Hoeben, P. Jonkheijm, E. W. Meijer, A. Schenning, *Chem. Rev.* **2005**, *105*, 1491; b) A. Ajayaghosh, V. K. Praveen, *Acc. Chem. Res.* **2007**, *40*, 644.

[2] a) A. M. van de Craats, J. M. Warman, K. Müllen, Y. Geerts, J. D. Brand, *Adv. Mater.* **1998**, *10*, 36; b) J.-F. Glowe, M. Perrin, D. Beljonne, L. Karsenti, S. C. Hayes, F. Gardebien, C. Silva in *Functional Supramolecular Architectures: For Organic Electronics and Nanotechnology, Vol. 2* (Eds.: P. Samori, F. Cacialli), Wiley-VCH, Weinheim, **2011**.

[3] a) M. A. Hempenius, B. M. W. Langeveld-Voss, J. van Haare, R. A. J. Janssen, S. S. Sheiko, J. P. Spatz, M. Moller, E. W. Meijer, *J. Am. Chem. Soc.* **1998**, *120*, 2798; b) S. A. Jenekhe, X. L. Chen, *Science* **1998**, *279*, 1903.

[4] a) J. S. Liu, E. Sheina, T. Kowalewski, R. D. McCullough, *Angew. Chem.* **2002**, *114*, 339; *Angew. Chem. Int. Ed.* **2002**, *41*, 329; b) M. F. Wang, D. L. Qiu, B. Zou, T. Wu, X. Zhang, *Chem. Eur. J.* **2003**, *9*, 1876; c) Y. H. Luo, H. W. Liu, F. Xi, L. Li, X. G. Jin, C. C. Han, C. M. Chan, *J. Am. Chem. Soc.* **2003**, *125*, 6447; d) H. B. Wang, W. You, P. Jiang, L. P. Yu, H. H. Wang, *Chem. Eur. J.* **2004**, *10*, 986; e) J. K. Kim, E. Lee, M. Lee, *Angew. Chem.* **2006**, *118*, 7353; *Angew. Chem. Int. Ed.* **2006**, *45*, 7195; f) A. L. Briseno, S. C. B. Mannsfeld, X. M. Lu, Y. J. Xiong, S. A. Jenekhe, Z. N. Bao, Y. N. Xia, *Nano Lett.* **2007**, *7*, 668; g) A. L. Briseno, S. C. B. Mannsfeld, C. Reese, J. M. Hancock, Y. Xiong, S. A. Jenekhe, Z. Bao, Y. Xia, *Nano Lett.* **2007**, *7*, 2847; h) J. Xiao, Z. Yin, H. Li, Q. Zhang, F. Boey, H. Zhang, Q. Zhang, *J. Am. Chem. Soc.* **2010**, *132*, 6926; i) B. Song, H. Wei, Z. Wang, X. Zhang, M. Smet, W. Dehaen, *Adv. Mater.* **2007**, *19*, 416; j) Y. S. Zhao, A. Peng, H. Fu, Y. Ma, J. Yao, *Adv. Mater.* **2008**, *20*, 1661; k) M. Yin, J. Shen, W. Pisula, M. Liang, L. Zhi, K. Müllen, *J. Am. Chem. Soc.* **2009**, *131*, 14618; l) A. J. J. V. Heyen, C. C. Buron, Q. Tianshi, R. Bauer, A. M. Jonas, K. Müllen, F. C. De Schryver, S. De Feyter, *Small* **2008**, *4*, 1160; m) V. Palermo, S. Morelli, C. Simpson, K. Müllen, P. Samori, *J. Mater. Chem.* **2006**, *16*, 266; n) M. Surin, P. Sonar, A. C. Grimsdale, K. Müllen, R. Lazzaroni, P. Leclère, *Adv. Funct. Mater.* **2005**, *15*, 1426.

[5] a) Y. Guo, H. Zhao, G. Yu, C.-a. Di, W. Liu, S. Jiang, S. Yan, C. Wang, H. Zhang, X. Sun, X. Tao, Y. Liu, *Adv. Mater.* **2008**, *20*, 4835; b) B. W. Messmore, J. F. Hulvat, E. D. Sone, S. I. Stupp, *J. Am. Chem. Soc.* **2004**, *126*, 14452; c) J. S. Wu, M. D. Watson, L. Zhang, Z. H. Wang, K. Müllen, *J. Am. Chem. Soc.* **2004**, *126*, 177; d) Y. Zhang, H. Dong, Q. Tang, S. Ferdous, F. Liu, S. C. B. Mannsfeld, W. Hu, A. L. Briseno, *J. Am. Chem. Soc.* **2010**, *132*, 11580; e) E. R. Zubarev, M. U. Pralle, E. D. Sone, S. I. Stupp, *J. Am. Chem. Soc.* **2001**, *123*, 4105; f) J. M. Mativetsky, M. Kastler, R. C. Savage, D. Gentilini, M. Palma, W. Pisula, K. Müllen, P. Samori, *Adv. Funct. Mater.* **2009**, *19*, 2486; g) D. Wu, L. Zhi, G. J. Bodwell, G. Cui, N. Tsao, K. Müllen, *Angew. Chem.* **2007**, *119*, 5513; *Angew. Chem. Int. Ed.* **2007**, *46*, 5417.

[6] a) J. P. Hill, W. S. Jin, A. Kosaka, T. Fukushima, H. Ichihara, T. Shimomura, K. Ito, T. Hashizume, N. Ishii, T. Aida, *Science* **2004**, *304*, 1481; b) Y. Yamamoto, T. Fukushima, Y. Suna, N. Ishii, A. Saeki, S. Seki, S. Tagawa, M. Taniguchi, T. Kawai, T. Aida, *Science* **2006**, *314*, 1761; c) Y. S. Zhao, J. Xu, A. Peng, H. Fu, Y. Ma, L. Jiang, J. Yao, *Angew. Chem.* **2008**, *120*, 7411; *Angew. Chem. Int. Ed.* **2008**, *47*, 7301.

[7] S. J. George, A. Ajayaghosh, P. Jonkheijm, A. Schenning, E. W. Meijer, *Angew. Chem.* **2004**, *116*, 3504; *Angew. Chem. Int. Ed.* **2004**, *43*, 3422.

[8] B. Song, Z. Q. Wang, S. L. Chen, X. Zhang, Y. Fu, M. Smet, W. Dehaen, *Angew. Chem.* **2005**, *117*, 4809; *Angew. Chem. Int. Ed.* **2005**, *44*, 4731.

[9] E. Lee, J. K. Kim, M. Lee, *Angew. Chem.* **2009**, *121*, 3711; *Angew. Chem. Int. Ed.* **2009**, *48*, 3657.

[10] a) D. J. Pochan, Z. Y. Chen, H. G. Cui, K. Hales, K. Qi, K. L. Wooley, *Science* **2004**, *306*, 94; b) S. Yagai, S. Mahesh, Y. Kikkawa, K. Unoike, T. Karatsu, A. Kitamura, A. Ajayaghosh, *Angew. Chem.* **2008**, *120*, 4769; *Angew. Chem. Int. Ed.* **2008**, *47*, 4691; c) S. Yagai, S. Kubota, H. Saito, K. Unoike, T. Karatsu, A. Kitamura, A. Ajayaghosh, M. Kanesato, Y. Kikkawa, *J. Am. Chem. Soc.* **2009**, *131*, 5408; d) S. Yagai, H. Aonuma, Y. Kikkawa, S. Kubota, T. Karatsu, A. Kitamura, S. Mahesh, A. Ajayaghosh, *Chem. Eur. J.* **2010**, *16*, 8652.

[11] W. Y. Yang, J. H. Ahn, Y. S. Yoo, N. K. Oh, M. Lee, *Nat. Mater.* **2005**, *4*, 399.

[12] A. Ajayaghosh, R. Varghese, V. K. Praveen, S. Mahesh, *Angew. Chem.* **2006**, *118*, 3339; *Angew. Chem. Int. Ed.* **2006**, *45*, 3261.

[13] a) G. Widawski, M. Rawiso, B. Francois, *Nature* **1994**, *369*, 387; b) S. A. Jenekhe, X. L. Chen, *Science* **1999**, *283*, 372; c) U. Stalmach, B. de Boer, C. Videlot, P. F. van Hutten, G. Hadziioannou, *J. Am. Chem. Soc.* **2000**, *122*, 5464; d) S. S. Babu, S. Mahesh, K. K. Kartha, A. Ajayaghosh, *Chem. Asian J.* **2009**, *4*, 824.

[14] a) M. Lee, B.-K. Cho, W.-C. Zin, *Chem. Rev.* **2001**, *101*, 3869; b) J. Qian, M. Zhang, I. Manners, M. A. Winnik, *Trends Biotechnol.* **2010**, *28*, 84; c) R. A. Segalman, B. McCulloch, S. Kirmayer, J. J. Urban, *Macromolecules* **2009**, *42*, 9205; d) S. I. Stupp, V. LeBonheur, K. Walker, L. S. Li, K. E. Huggins, M. Keser, A. Amstutz, *Science* **1997**, *276*, 384.

[15] a) F. S. Bates, G. H. Fredrickson, *Annu. Rev. Phys. Chem.* **1990**, *41*, 525; b) L. F. Zhang, A. Eisenberg, *Science* **1995**, *268*, 1728.

[16] H.-J. Kim, T. Kim, M. Lee, *Acc. Chem. Res.* **2011**, *44*, 72.

[17] a) M. Smet, J. Van Dijk, W. Dehaen, *Synlett* **1999**, 495; b) A. R. Mohebbi, F. Wudl, *Chem. Eur. J.* **2011**, *17*, 2642.

[18] A. R. Mohebbi, J. Yuen, J. Fan, C. Munoz, M. F. Wang, R. S. Shirazi, J. Seifter, F. Wudl, *Adv. Mater.* **2011**, *23*, 4644.

[19] S. S. Babu, S. Prasanthkumar, A. Ajayaghosh, *Angew. Chem.* **2012**, *124*, 1800; *Angew. Chem. Int. Ed.* **2012**, *51*, 1766.

[20] By Image J, a Java-based image processing program developed at the National Institutes of Health.

[21] R. D. Deegan, O. Bakajin, T. F. Dupont, G. Huber, S. R. Nagel, T. A. Witten, *Nature* **1997**, *389*, 827.

[22] W. Han, Z. Lin, *Angew. Chem.* **2012**, *124*, 1566; *Angew. Chem. Int. Ed.* **2012**, *51*, 1534.

[23] J. N. Israelachvili, *Intermolecular and Surface Forces*, Elsevier, Amsterdam, **2011** (where μ_N is the standard part of the chemical potential (the mean interaction free energy per molecule) in aggregates of aggregation number N; μ_∞ is the "bulk" energy of a molecule in an infinite aggregate; α is a positive constant dependent on the strength of the intermolecular interactions; T is temperature (K); k is Boltzmann constant; p is a number that depends on the shape or dimensionality of the aggregates.).

[24] N. K. Raman, M. T. Anderson, C. J. Brinker, *Chem. Mater.* **1996**, *8*, 1682.

[25] J. M. Schnur, B. R. Ratna, J. V. Selinger, A. Singh, G. Jyothi, K. R. K. Easwaran, *Science* **1994**, *264*, 945.

[26] Y. Y. Won, H. T. Davis, F. S. Bates, *Science* **1999**, *283*, 960.

[27] a) D. R. M. Williams, G. H. Fredrickson, *Macromolecules* **1992**, *25*, 3561; b) S. Lin, N. Numasawa, T. Nose, J. Lin, *Macromolecules* **2007**, *40*, 1684.

